Mesenchymal stem cells derived from CHIR99021 and TGF-β induction remained on the colicomentum and improved cardiac function of a rat model of acute myocardium infarction

YUSEN ZHANG[1*], YANMIN ZHANG[2*], AZHEN HU[3], FANHUA MENG[4], PENG CUI[5], TIANSHI LI[6] and GUANGHUI CUI[2]

[1]Department of Ultrasound; [2]Central Laboratory, Peking University Shenzhen Hospital; [3]Shenzhen Key Laboratory of Drug Addiction and Safe Medication, Shenzhen PKU-HKUST Medical Centre; [4]Reproductive Medical Centre; [5]Institute of Precision Medicine; [6]Department of Plastic Surgery, Peking University Shenzhen Hospital, Shenzhen, Guangdong 518036, P.R. China

Received July 3, 2023; Accepted January 17, 2024

DOI: 10.3892/etm.2024.12470

Abstract. Human induced pluripotent stem cells (hiPSCs) have been regarded as a potential stem cell source for cell therapy. However, the production of cells with mesenchymal potential from hiPSCs through spontaneous differentiation is time consuming and laborious. In the present study, the combined use of the GSK-3 inhibitor CHIR99021 and TGF-β was used to obtain mesenchymal stem cell (MSC)-like cells from hiPSCs. During the induction process, the transcription of epithelial-mesenchymal transition (EMT)-related genes N-cadherin and Vimentin in the transformed cells was upregulated, whereas the transcription of E-cadherin and pluripotency-related transcription factors *SOX2, OCT4* and *NANOG* did not change significantly. This indicated that whilst cells were pluripotent, EMT was initiated by the upregulation of transcription of EMT promoting genes. Both SMAD-dependent and independent signalling pathways were significantly activated by the combined induction treatment compared with the single factor induction. The hiPSC-derived MSC-like cells (hiPSC-MSCs) expressed MSC-related markers and acquired osteogenic, chondrogenic and adipogenic differentiation potentials. After being injected into the peritoneal cavity of rats, the hiPSC-MSCs secreted angiogenic and immune-regulatory factors and remained on the colicomentum for 3 weeks. Within an 11-week period, four intraperitoneal hiPSC-MSC injections ($1x10^7$ cells/injection) into acute myocardial infarction (AMI) model rats significantly increased the left ventricular ejection fraction, left ventricular fractional shortening and angiogenesis and significantly reduced scar size and the extent of apoptosis in the infarcted area compared with that of the control PBS injection. Symptoms of hiPSC-MSC-induced immune reaction or tumour formation were not observed over the course of the experiment in the hiSPC-MSC treated rats. In conclusion, the CHIR99021 and TGF-β combined induction was a rapid and effective method to obtain MSC-like cells from hiPSCs and multiple high dose intraperitoneal injections of hiPSC-derived MSCs were safe and effective at restoring cardiac function in an AMI rat model.

Correspondence to: Dr Guanghui Cui, Central Laboratory, Peking University Shenzhen Hospital, 1120 Lianhua Road, Futian, Shenzhen, Guangdong 518036, P.R. China
E-mail: cuiguanghui@pkuszh.com

Dr Tianshi Li, Department of Plastic Surgery, Peking University Shenzhen Hospital, 1120 Lianhua Road, Futian, Shenzhen, Guangdong 518036, P.R. China
E-mail: tianshi8811520@163.com

*Contributed equally

Key words: mesenchymal stem cell, human induced pluripotent stem cell, epithelial-to-mesenchymal transition, peritoneal injection, acute myocardial infarction, cardiac function

Introduction

Mesenchymal stem cells (MSCs) are immunologically tolerable cells that exhibit low expression levels of major histocompatibility complex (MHC) I and negligible expression levels of MHC II and co-stimulatory molecules B7-1, B7-2, CD40 or CD40L (1). Through direct interactions with target cells or paracrine signalling molecules, such as indoleamine 2, 3 dioxygenase, prostaglandin E2 (PGE2) and IL-10, MSCs exert regulatory effects on immune cell activation (1). Previous studies have reported that the therapeutic functions of transplanted MSCs is based on the secretion of angiogenesis stimulating and inflammatory alleviating factors (2-6), therefore, MSC injection has been widely used in the treatment of ischemic heart disease (7-9).

MSCs reside in various adult tissues (10); however, MSC populations isolated from these tissues are heterogeneous and MSC preparations are also affected by the type of tissue that these cells are isolated from and the age of donor (11,12). MSC proliferation capacity decreases with donor age and multiple rounds of *in vitro* culture expansion can cause replicative senescence and a change in cell function (12). Furthermore,

the potency of human MSCs is limited compared with that of embryonic stem cells (ESCs) or induced pluripotent stem cells (iPSCs). Therefore, obtaining MSCs with enhanced proliferation and differentiation potentials to improve their clinical utility is of primary importance for their use to treat certain diseases.

Currently, stem cell derived MSCs are regarded as an important cell source to replace tissue derived MSCs. Given that human ESCs are derived from human embryos, there are ethical issues associated with using human ESCs as therapeutic cell source. However, the application of human somatic cell derived iPSCs (hiPSCs) for patient-specific autologous regenerative treatment is promising with fewer ethical concerns, and differentiating hiPSCs into multipotent progenitors prior to transplantation is one of the most suitable, safe and effective approaches for the use of iPSCs (13). This approach could eliminate the issue of immune incompatibility and provide a unified starting point for generating high quality iPSC derived MSCs at a large scale (13).

Epithelial-mesenchymal transition (EMT) is a biological process in embryonic development that serves an important role in human ESC mesoderm commitment (13). hiPSC spontaneous mesoderm differentiation can be initiated by subsequent passaging of cells at a low cell density or during cell embryoid body formation. A time period of ≥30 days is required to produce cells with increased expression levels of MSC markers. Hence, there is an urgent need to develop a more rapid method of obtaining MSCs from hiPSCs, such as prompting EMT though the addition of soluble active agents.

TGF-β is a secreted growth and differentiation factor that exerts a verity of biological activities depending on the type of cellular target. During the process of embryonic development, TGF-β expression is often detected at the site of epithelial and mesenchymal interaction (14). TGF-β, through binding with its receptor, activates a series of intracellular signal transduction factors, including sentinel node invasion level 1/2 and zinc finger E-box binding homeobox 1/2, which promote epithelial cell EMT by upregulating the mesenchymal specification related marker N-cadherin (15,16).

GSK-3 was initially reported to be a glycogen synthase inhibitor. However, additional studies have since reported that GSK-3 was involved with the regulation of >100 substrates (17,18). Previously, it was reported that SNAIL repressed the expression of E-cadherin and induced EMT as constitutive activation of GSK-3 induced SNAIL degradation and stabilization of SNAIL through inhibition of GSK-3β resulted in suppression of E-cadherin expression during TGF-β induced EMT (19,20). After co-culturing with *Xenopus tropicalis* immature Sertoli cells for 3 days, the GSK-3 inhibitor CHIR99021 increased the expression of EMT transcription factors and the number of cells with an MSC-like morphology (21).

To date, a number of reports indicate that the experimental and clinical studies using MSCs to treat myocardium infarction have used an intramyocardial or intracoronary cell delivery system (7-9). However, the operation of intramyocardial or intracoronary cell delivery is complicated and invasive, as a result, repeated intromyocardial or introcoronary cell delivery is not acceptable for most of these patients (22). In comparison with intramyocardial or intracoronary cell delivery, it is more convenient for patients to be administered with multiple intravenous (IV) MSC injections. Nevertheless, it has been reported that only a small portion of the injected cells integrate into the infarcted area, as most of the injected cells were found in lung, kidney, liver or spleen tissues and have the potential to form lethal thromboemboli in these organs (22,23).

The peritoneal cavity is also an appropriate place for cell injection because there are active fluid and cellular exchanges occurring between the cavity and the general circulatory system (23,24). The exchange takes place through three possible channels: i) 'Milky spots', which are located on the surface of the colicomentum and the fatty tissues; ii) the draining lymphatic system; and iii) punctate regions (24). Intraperitoneal (IP) injection permits the administration of higher cell doses without causing embolization in any organs (24). In addition, IP injections of MSCs were reported to have more beneficial effects compared with IV injections in the treatment of experimental autoimmune encephalomyelitis, cisplatin-induced renal injury, cornea sterile inflammation and zymosan-induced peritonitis (25-30).

EMT can be initiated by activation of multiple extracellular signals, including the TGF-β superfamily and the Wnt signalling pathway (14,15,18,19). In the present study, the combined treatment of GSK-3 inhibitor CHIR99021 and TGF-β was tested to determine if this treatment would promote hiPSC EMT and facilitate the derivation of MSCs. Secondly, the hiPSC derived MSCs (hiPSC-MSCs) were intraperitoneally administrated into a rat model of acute myocardial infarction (AMI) at a high dosage to evaluate the safety and efficacy of hiPSC-MSCs for the treatment of a rat model of AMI.

Materials and methods

hiPSC cell line and culture. The hiPSC cell line PBMC-5 (at passage 10) was donated by Dr Tiancheng Zhou. hiPSCs were prepared from peripheral blood mononuclear cells of a healthy Han Chinese female donor (age, 31 years) in CAS Key Laboratory of Regenerative Biology, Guangzhou Institutes of Biomedicine and Health (Guangzhou, China). Cells were separated using a Ficoll-Paque gradient (Shenzhen DAKEWE Bio-Engineering Co., Ltd.) and reprogramed using the CTS™ CytoTune™-iPS Sendai virus reprograming kit (Thermo Fisher Scientific, Inc.). The hiPSCs were maintained as large cell colonies on Matrigel-coated plates (BD Biosciences) in serum free mTeSR1 medium (STEMCELL Technologies) at 37˚C, in 5% CO_2.

MSC differentiation of hiPSCs. Dispersed single hiPSC cells at passage 15 were seeded onto a Matrigel-coated 12-well plate in mTeSR1 medium at a density of $2x10^4$ cells/cm^2 2 days before induction. Cells were treated with the following different MSC differentiation mediums for 6 days: i) DMEM basal medium supplemented with 10% knockout serum replacement (Invitrogen; Thermo Fisher Scientific, Inc.), 1 mM L-glutamine, 10 mM non-essential amino acids, 50 U/ml penicillin/streptomycin (Invitrogen; Thermo Fisher Scientific, Inc.) and 0.5 μl/ml DMSO (MilliporeSigma; Merck KGaA); ii) DMEM containing 5 or 10 μM CHIR99021 (Stemgent, Inc.; REPROCELL), iii) DMEM containing 10 or 20 μg/ml TGF-β (Creative BioMart); or iv) DMEM medium containing 5 μM

CHIR99021 and 10 μg/ml TGF-β. The selected concentrations of CHIR99021 and TGF-β used in the present study were selected on the basis of previous reports (20,30-33) and the induction medium was changed every other day.

At 6 days after cell induction, the differentiated cells were dispersed into single cells through TrypleSelect (Invitrogen; Thermo Fisher Scientific, Inc.) digestion at 37˚C for 5 min and collected by centrifugation at 500 x g for 5 min. The collected cells were suspended in MSC medium [DMEM basal medium supplemented with 10% FBS (HyClone; Cytiva), 1 mM L-glutamine, 50 U/ml penicillin/streptomycin and 10 mM non-essential amino acids (Invitrogen; Themo Fisher Scientific, Inc.)] and seeded at a density of $4x10^4$ cells/cm^2. In subsequent passages, the cell concentration was reduced to $2x10^4$ cells/cm^2. The cell induction experiment was repeated thrice.

Reverse transcriptase-quantitative PCR (RT-qPCR). Total RNA isolation from the induced cells was conducted using the RNase mini kit (Qiagen, Inc.) and a high-capacity RNA-to-cDNA kit (Applied Biosystems; Thermo Fisher Scientific, Inc.) was used to reverse transcribe RNA into cDNA according to the manufacturer's instructions (incubation at 85˚C for 5 sec and 37˚C for 1 h). For quantification of gene expression, RT-qPCR was performed using specific primers (Table I) and SYBR-Green RT-PCR reagents (Applied Biosystems; Thermo Fisher Scientific, Inc.) under the following thermocycling conditions: denaturation at 94˚C for 30 sec; annealing at 60˚C for 35 sec and extension at 72˚C for 40 sec, 30 cycles. The $2^{-\Delta\Delta Cq}$ method was used to analyse relative gene expression levels and GAPDH was used as the normalisation control (34). The quantification of gene transcription was repeated three times.

Western blotting. The EpiQuik whole cell extraction kit (AmyJet Scientific, Inc.) was used to extract total protein from the induced cells and protein concentration was measured using the Bradford DC protein assay (Bio-Rad Laboratories). Protein samples (30 μg) were separated by electrophoresis on 12% Bis-Tris polyacrylamide gel and then transferred to nitrocellulose membranes (MilliporeSigma; Merck KGaA). The membranes were blocked with 5% BSA (Wuhan Servicebio Technology Co., Ltd.) at room temperature for 1.5 h and incubated overnight at 4˚C with the following primary antibodies: SMAD 2/3 (cat. no. #3102S), ERK1/2 (cat. no. #4695T) (Cell Signalling Technology, Inc.), GSK-3 (cat. no. #PA532440; Thermo Fisher Scientific, Inc.) and SNAIL (cat. no. #ABD38; MilliporeSigma) primary antibodies at 1:1,000 dilution at 4˚C for 12 h, followed by incubation with goat anti-rabbit polyclonal HRP conjugated secondary antibodies (1:10,000 dilution in 1% milk/TBS; cat. no. #A16110; Thermo Fisher Scientific, Inc.) for 2 h at room temperature. Protein bands were visualized using a chemiluminescence detection kit (Amersham; Cytiva) and analyzed using Tanon 5220S image analysis system (Tanon Image software version 1.0; Tanon Science and Technology Co., Ltd.). Analysis of protein expression levels was repeated thrice.

MSC specific marker detection and cell differentiation assay. At six passages after the initial MSC induction from hiPSCs, the adherent cells with a spindle-like morphology were collected by 0.25% trypsin treatment at 37˚C for 5 min and centrifugation at 500 x g for 5 min. Then the cells were resuspended in PBS at $1x10^6$ cells/ml for determining the expression levels of typical MSC surface markers (CD29, CD44, CD73, CD90 and CD105) and hematopoietic cell lineages markers [CD34, CD45 and human leukocyte antigen-DR isotype (HLA-DR)] by fluorescence-activated cell sorting. The antibodies used were as follows: fluorescent conjugated anti-CD29, -CD44, -CD73, -CD90 and -CD105 antibodies (cat. nos. #354603, #338807, #344003, #328109 and #323205, respectively; BioLegend, Inc.); primary anti-CD45, -CD34, -HLA-DR antibody and CY3 conjugated goat anti-rabbit IgG secondary antibody (cat. nos. #A0055-3, #BM4082, #BM4546 and #BA1032, respectively; Wuhan Boster Biological Technology, Ltd.). The primary antibodies (1:200 dilution) and secondary antibody (1:5,000 dilution) were incubated respectively with the cells for 30 min at room temperature, and then the cell surface marker expression was measured by BD-FACScan (Becton, Dickinson and Company), and the data were analysed using FlowJo (V10; FlowJo LLC). Measurements were repeated three times.

The induction of osteogenic, chondrogenic and adipocytic differentiation and subsequent evaluation of the induced cells was conducted as previously described (33). Osteogenic differentiation was initiated by culturing cells with osteo-inductive medium [DMEM basal medium supplemented with 10% FBS (HyClone; Cytiva), 10 mM glycerol phosphate, 50 μM ascorbate phosphate, 10^{-7} M dexamethasone (MilliporeSigma; Merck KGaA) and 100 ng/ml recombinant human bone morphogenic protein-2 (Invitrogen; Thermo Fisher Scientific, Inc.)] for 2 weeks. For chondrogenic differentiation, cells were cultured in chondrogenic induction medium [DMEM basal medium supplemented with 10% FBS, 6.25 μg/ml of insulin (Fisher Scientific, Thermo Fisher Scientific, Inc.), 50 nM of ascorbate phosphate and 10 ng/ml of TGF-β] for 2 weeks.

Table I. Primers used for reverse transcriptase-quantitative PCR.

Gene	Sequence (5'-3')
E-cadherin	F: TTCTGCTGCTCTTGCTGTTT
	R: TGGCTCAAGTCAAAGTCCTG
N-cadherin	F: CCTGCGCGTGAAGGTTTGCC
	R: CCAAGCCCCGCACCCACAA
Vimentin	F: GCCCTTAAAGGAACCAATGA
	R: AGCTTCAACGGCAAAGTTCT
Oct3/4	F: GACAGGGGGAGGGGAGGAGCTAGG
	R: CTTCCCTCCAACCAGTTGCCCCAAAC
Sox2	F:GGGAAATGGGAGGGGTGCAAAAGAGG
	R: TTGCGTGAGTGTGGATGGGATTGGTG
Nanog	F: CAGCCCCGATTCTTCCACCAGTCCC
	R: CGGAAGATTCCCAGTCGGGTTCACC
GAPDH	F: CATCAATGGAAATCCCATCA
	R: TTCTCCATGGTGGTGAAGAC

F, forward; R, reverse.

The adipocytic differentiation potential was analysed using adipogenic induction medium (DMEM supplemented with 10% FBS, 10^{-7} M of dexamethasone and 10 μg/ml of insulin) to culture the cells for ≥2 weeks.

The cells growing on 60 mm culture dish (Corning) were fixed by 4% formaldehyde for 10 min at room temperature, and then stained respectively by 0.1% Alizarin red, 1% Alcian blue and 0.5% Oil-Red-O at room temperature for 30 min to visualize calcium nodule formation, sulphated proteoglycan formation and intracellular lipid accumulation in the cells under light microscope at magnification x200 (Olympus).

Animal acute myocardium infarction (AMI) model. A total of 30 male Wister rats (age, 4 weeks; weight, 230-270 g) were purchased from The Medical Experimental Animal Centre of Guangdong Province. The rats were housed under constant 20˚C temperature, 45% humidity and a 12 h light-dark cycle and had free access to standard laboratory chow and tap water.

Approval for the animal experimentation was granted by The Animal Ethics Committee of The Peking University & Hong Kong Science and Technology University Medical Centre (approval no. 2020-027). Chinese laws relating to the care and treatment of animals and the Animal Research: Reporting of In Vivo Experiments guidelines were followed throughout the study (35).

The rats were randomly separated into MSC injection group, PBS injection group and sham group, with 10 rats in each group. In order to construct the AMI model, rats were first anaesthetised by pentobarbital sodium (40 mg/kg) intraperitoneal injection and then the heart was exposed via a left thoracotomy between the 4th and 5th ribs of the animal. A tight suture was made around the left anterior descending coronary artery and the resulted ischemia was maintained for 40 min and then the suture was removed to restore blood flow. In the sham control group, the suture was immediately removed without any further maintaining.

Before sacrifice, the rats were administered an IP injection of pentobarbital sodium (40 mg/kg). When the rats were anaesthetised and unresponsive to stimuli, cervical dislocation was used to sacrifice each animal. In order to confirm death, the absence of breath sounds and heart beat was monitored by observation and echocardiography.

IP administration and distribution of hiPSC-MSCs in AMI model rats. Immediately after AMI, model rats were divided randomly into hiPSC-MSC injection group (n=10) and PBS injection control groups (n=10). An IP injection of $1x10^7$ hiPSC-MSCs (passage 6 after the initial MSC induction from hiPSC) was administered to rats in the hiPSC-MSC treated group each week for 4 weeks, with PBS injections used as a control.

To determine the distribution of the IP injected hiPSC-MSCs, $1x10^7$ hiPSC-MSCs were labelled with Xeno Light Dir (PerkinElmer, Inc.) and injected into the peritoneal cavity of rats (n=3). The signals of the injected cells were detected using the Lumina IVIS II System (PerkinElmer, Inc.) and the fluorescence images of the peritoneal cavity and individual colicomenta were obtained using the Living Image Software (version 4.1; PerkinElmer, Inc.) immediately after the injection, 3 days after the injection, 1 week after the injection and 3 weeks after the injection.

Peritoneal lavage fluid cytokine analysis. For *in vivo* cytokine assay analysis, 1 week after the IP cell injection, 10 ml of PBS was injected into the peritoneal cavity of the anesthetised (40 mg/kg pentobarbital sodium) hiPSC-MSC injected (n=3) and control rats (n=3) with a 10-gauge syringe and the peritoneal lavage was collected. The concentrations of insulin-like growth factor (IGF), VEGF, hepatocyte growth factor (HGF), prostaglandin E2 (PGE2), IL-4 and IL-10 in the lavage were measured using ELISA kits following the manufacturer's instructions. The kits used were as follows: Human IGF-1 ELISA kit (cat. no. #EK1131-48), PGE2 Competitive ELISA kit (cat. no. #EK8103/2-48) (Hangzhou Lianke Biotechnology Co., Ltd.), human VEGF ELISA Kit (cat. no. #ab100663), hepatocyte growth factor ELISA kit (cat. no. #ab275901) (Abcam), human IL-10 ELISA kit (cat. no. KIT10947A), human IL-4 ELISA kit (cat. no. KIT11846) (Sinopharm Chemical Reagent Co., Ltd.). A 1510 spectrophotometer (Thermo Fisher Scientific, Inc.) was used to analyse the samples and the measurements were repeated three times.

Echocardiography evaluation of cardiac function. A 2D echocardiography system (Vevo 2100; Visual Sonics) with a MS250 transducer (13-24 MHz) was used to evaluate the cardiac function of the AMI model rats. The parameter changes pertaining to left ventricular ejection fraction (LVEF) and left ventricular fractional shortening (LVFS) were measured and analysed.

Scar size quantification. The area of myocardial scars of the AMI model rats was assessed using Masson's trichrome staining 11 weeks after AMI induction. Briefly, tissue sections of the infarcted area were fixed in 4% formaldehyde, embedded in paraffin and cut into 5 μm slices. The slices were stained with Masson's trichrome to detect fibrosis and three tissue slices taken from each rat were assessed by a pathologist who was blinded to the samples. The scar area percentage of total tissue area was quantified using a computerised morphometry system with a light microscope (Cell Sens; Ver.1.16; Olympus Corporation).

Infarcted area vascularisation evaluation. Heart tissue was fixed with 4% paraformaldehyde (Beyotime Institute of Biotechnology) for 72 h at room temperature, embedded in paraffin and cut into sections (4 μm). Tissue slices (n=3) from each rat were deparaffinized, rehydrated and pressure-cooked at 121˚C for 4 min in citrate buffer (10 mM, pH 6.0) for antigen retrieval. The sections were incubated in 1% H_2O_2/methanol at room temperature for 10 min and then blocked in 4% bovine serum (Invitrogen; Thermo Fisher Scientific, Inc.) for 30 min at room temperature. Immunohistochemistry detection of α-SMA expressing cells was conducted with primary mouse anti-rat α-SMA antibodies (1:50 dilution; incubation 2 h at 4˚C; cat. no. #614852; BioLegend, Inc.) and secondary HRP conjugated anti-mouse IgG antibodies (1:100 dilution, incubation 30 min at room temperature, Wuhan Boster Biological Technology, Ltd. Cat.# BA1051). α-SMA positive capillaries in the infarcted regions were manually counted under light microscope using high-power fields (hpf) of magnification (x200) in each tissue section.

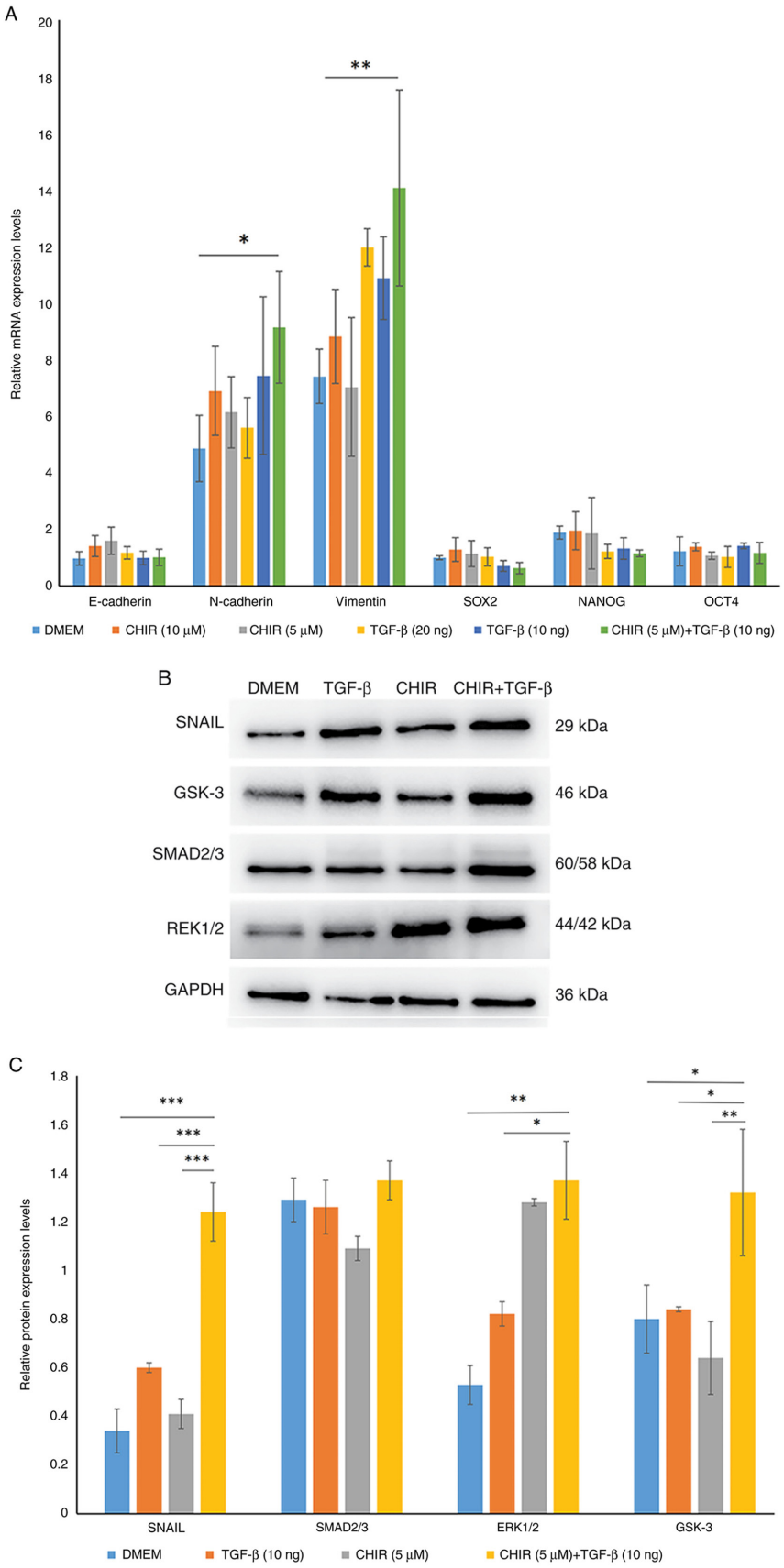

Figure 1. CHIR99021 and TGF-β treatment promoted EMT of human iPSCs. (A) Treatment of iPSCs with CHIR99021, TGF-β or CHIR99021 + TGF-β markedly upregulated the expression of EMT-related genes N-cadherin and Vimentin compared with untreated controls. Significant upregulation of N-cadherin was demonstrated in the CHIR99021 + TGF-β treated cells compared with untreated controls. The expression levels of E-cadherin, Oct4, Sox2 and Nanog were not significantly altered. (B) Treatment of cells with CHIR99021, TGF-β or CHIR99021 + TGF-β increased the protein expression levels of ERK1/2, SNAIL and GSK-3 in the transformed cells compared with control cells. (C) In comparison with the untreated and TGF-β treated cells, the protein expression levels of ERK1/2, SNAIL and GSK-3 in CHIR99021 + TGF-β treated cells was significantly increased. *P<0.05, **P<0.01, ***P<0.001. CHIR, CHIR99021; iPSC, induced pluripotent stem cells; EMT, epithelial-mesenchymal transition.

Apoptosis assay. To quantify the extent of cardiomyocyte apoptosis, a TUNEL kit (Nanjing KeyGen BioTech Co., Ltd.) was used to stain apoptotic cells present in heart tissue sections (prepared the same way as in the scar size quantification) according to the manufacturer's recommendations. 0.5% Hematoxylin counterstaining was conducted to better visualize normal nuclei. Apoptotic cells were counted in 5 randomly selected hpf of magnification (x400) in the infarcted area of three tissue sections from each rat and the mean count calculated.

Statistical analysis. Data were presented as mean ± standard deviation and analysed using GraphPad Prism (version 5; GraphPad; Dotmatics). A one-way ANOVA with Dunnett's test was used for multiple comparisons and an unpaired t-test was used for comparisons between two groups. $P<0.05$ was considered to indicate a statistically significant difference.

Results

CHIR99021 and TGF-β treatment promoted EMT of human iPSCs. To examine whether CHIR99021 or TGF-β treatment could initiate mesoderm commitment, hiPSCs were treated with CHIR99021, TGF-β or a CHIR99021 + TGF-β combination for 6 days. The mRNA expression levels of EMT-related genes N-cadherin and Vimentin, mesenchymal to epithelial transition (MET)-related gene E-cadherin and pluripotency-related transcription factors *OCT4, SOX2* and *NANOG* were evaluated using RT-qPCR (Fig. 1A).

After treatment with CHIR99021, TGF-β or the CHIR99021 + TGF-β combination for 6 days, compared with the untreated control cells, the mRNA expression levels of EMT related genes N-cadherin and Vimentin in the CHIR99021 or TGF-β treated cells was markedly upregulated and significant upregulation was demonstrated in the 5 μM CHIR99021 +10 μg/ml TGF-β treated cells (N-cadherin, $P<0.05$; Vimentin, $P<0.01$). A decrease in the cell growth rate and apoptosis were observed when the concentration of CHIR99021 and TGF-β was increased to 10 μM and 20 μg/ml, respectively (data not shown). As a result, the combination of 5 μM CHIR99021 +10 μg/ml TGF-β was used in the subsequent experiments. The mRNA expression levels of *OCT4, SOX2, NANOG* and E-cadherin in the CHIR99021 or TGF-β treated cells were not significantly altered compared with that of the untreated control cells.

To further investigate the potential mechanism involved in the CHIR99021 and TGF-β induced EMT of hiPSCs, analysis of SNAIL, SMAD2/3, ERK1/2 and GSK-3 protein expression levels was conducted by western blotting in the control, CHIR99021, TGF-β and CHIR99021 + TGF-β treated hiPSCs (Fig. 1B and C). These results demonstrated that after 6 days of induction, the protein expression levels of SNAIL and ERK1/2 in the 5 μM CHIR99021 +10 μg/ml TGF-β treated cells were significantly increased compared with that of the DMEM or single reagent treated cells. There was no significant difference in the protein expression levels of SMAD2/3 in control and treated cells. Furthermore, CHIR99021 + TGF-β treatment significantly increased the GSK-3 protein expression levels compared with the control and single reagent treatments.

Morphology, surface-marker expression and differentiation of hiPSC-MSCs. The morphology of hiPSC-MSCs was analysed (Fig. 2A). At passage 3, the spontaneously differentiating cells mainly had a pleomorphic morphology. In the cells treated with 10 or 20 μg/ml TGF-β, <20% of cells exhibited a short spindle and olive-shaped morphology. In the cells treated with 5 μM CHIR99021, >30% of the cells exhibited a short spindle shape, whereas in the 10 μM CHIR99021 treated cells, the percentage of spindle shaped cells was close to 50%. In cells treated with 5 μM CHIR99021 +10 μg/ml TGF-β, ≥70% of the adherent cells exhibited a spindle-shaped morphology.

MSC surface marker expression and osteogenic, chondrogenic and adipogenic differentiation analysis was conducted on the cells at passage 6. MSC surface marker expression analysis demonstrated that >90% of cells expressed typical MSC surface markers (CD29, CD44, CD73, CD90 and CD105), while the percentage of cells expressing hematopoietic cell lineage markers (CD34, CD45 and HLA-DR) was ≤0.6% (Fig. 2B).

After 2 weeks osteogenic, chondrogenic and adipogenic differentiation, alizarin red staining positive calcium nodules and alcian blue staining positive sulphated proteoglycans were detected in osteogenic and chondrogenic differentiating cells respectively. In adipogenic differentiated cells, intercellular lipid vacuoles were identified by Oil-Red-O staining. No typical positive stained cell was found among the three corresponding un-induced control cells (Fig. 2C).

IP injected hiPSC-MSCs remained on the colicomentum and produced angiogenic and immune regulatory factors. The distribution of hiPSC-MSCs was monitored after IP injection (Fig. 3A). At 1 h after the labelled hiPSC-MSCs injection, the fluorescent signal was detected around the injection site and 3 days after cell injection, the fluorescent signal moved from the injection site to colicomentum. Fluorescent signals could be detected for up to 3 weeks on the colicomentum and no fluorescent signals were detected in the liver, spleen or kidneys. There was no obvious evidence of an associated inflammatory response or tumour formation in the peritoneal cavity.

Angiogenic and immune regulatory factors were measured 1 week after hiPSC-MSC injections using the peritoneal lavage of hiPSC-MSC injected rats and control rats (Fig. 3B). The levels of IGF, VEGF, HGF, PGE2, IL-4 and IL-10 in the lavage of hiPSC-MSC injected rats were significantly increased compared with that in the control rats.

hiPSC-MSC injections improved cardiac function and survival of AMI model rats. Cardiac function was monitored by measuring LVEF and LVFS at 2-week intervals from the initial hiPSC-MSC injection to the end of the experiment. Representative echocardiogram images taken 11 weeks after AMI was induced demonstrated that the parameters reflecting the structure and function of heart such as anterior and posterior wall thickness, ventricular dimension enlargement and ventricular contraction of the sham group remained normal (Fig. 4A-a). In the PBS injection group, anterior and posterior wall thickness, ventricular dimension enlargement and ventricular contraction decrease were demonstrated (Fig. 4A-b), whereas in the hiPSC-MSC injection group, anterior and posterior wall thickness, ventricular dimension enlargement and ventricular contraction decrease were improved compared with that of the PBS injection group (Fig. 4A-c).

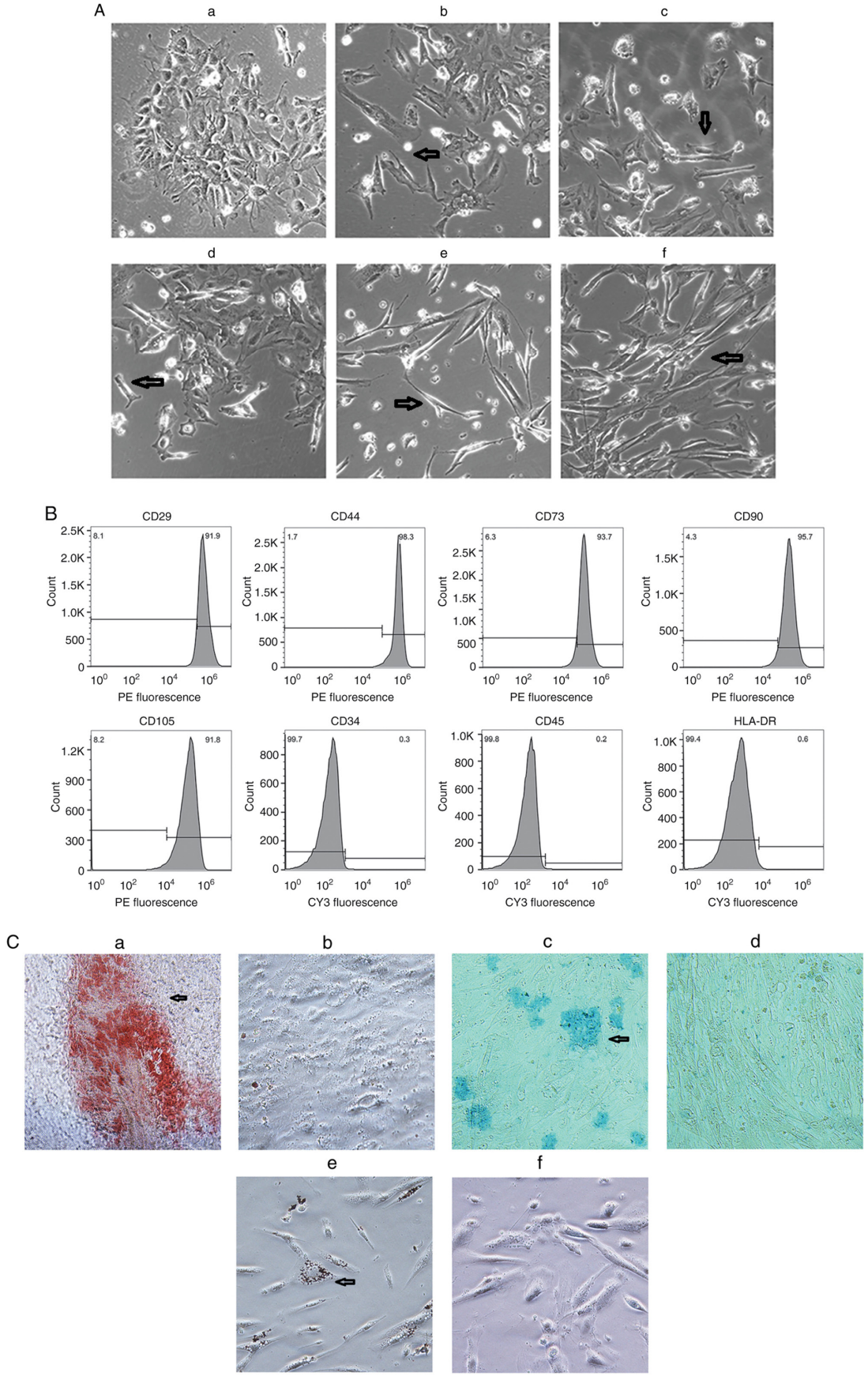

Figure 2. Cell morphology, surface-marker expression and differentiation of hiPSC-MSCs. (A) Cells with spindle morphology appeared (arrow) at passage 3 in cells treated with (A-a) DMEM, (A-b) TGF-β (20 μg/ml), (A-c) TGF-β (10 μg/ml), (A-d) CHIR99021 (10 μM), (A-e) CHIR99021 (5 μM) and (A-f) CHIR99021 (5 μM)+TGF-β (10 μg/ml). Magnification, x100. (B) Surface-marker expression analysis demonstrated >90% of cells expressed typical MSC surface markers (CD29, CD44, CD73, CD90 and CD105), whilst ≤0.6% of cells expressed hematopoietic cell lineage markers (CD34, CD45 and HLA-DR). (C) hiPSC-MSCs demonstrated (C-a) osteogenic, (C-c) chondrogenic and (C-e) adipogenic differentiation, whereas uninduced cells (C-b, C-d and C-f) did not. Magnification, x400. hiPSC-MSCs, human induced pluripotent stem cells-mesenchymal stem cells; HLA-DR, human leukocyte antigen-DR isotype.

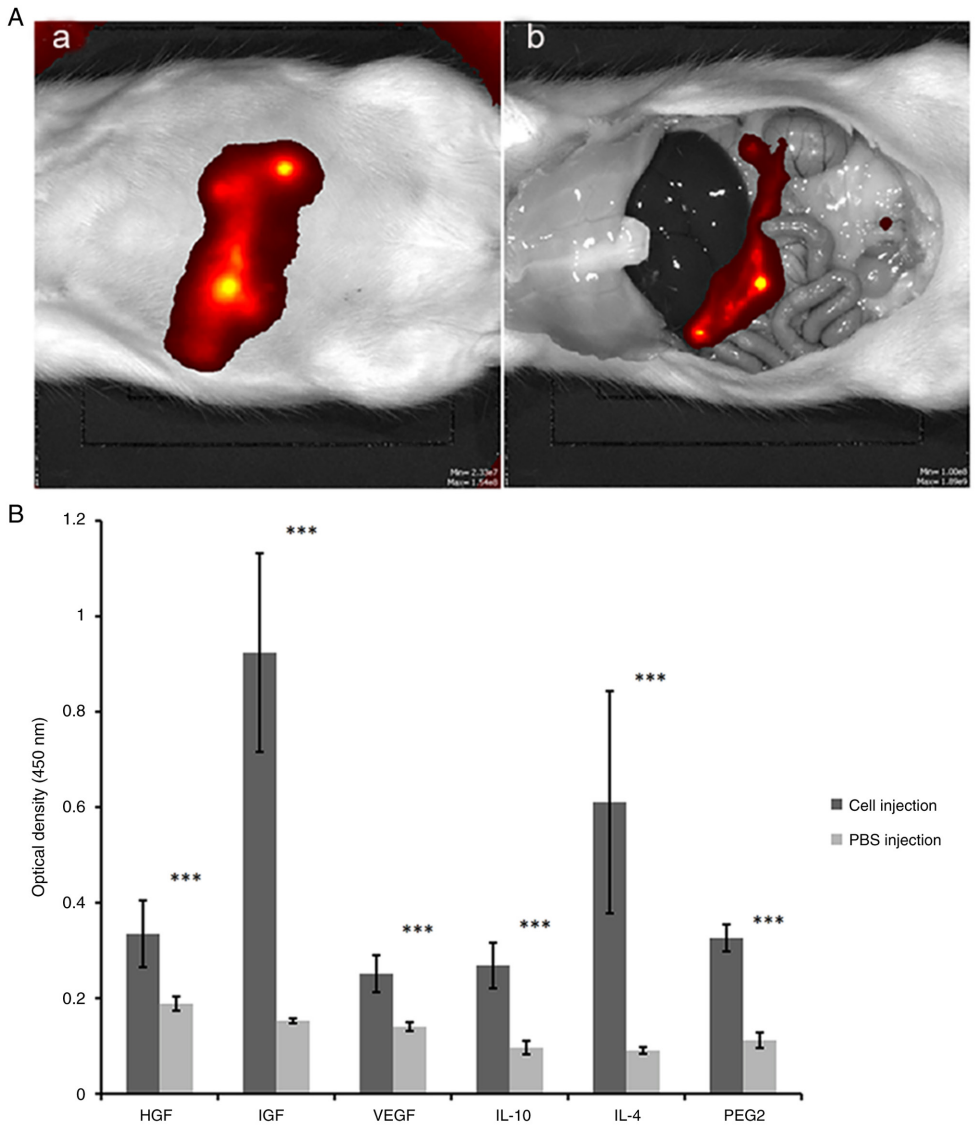

Figure 3. Intraperitoneally injected hiPSC-MSCs remained on the colicomentum and produced angiogenic and immune regulatory factors. (A) Cell distribution analysis demonstrated that signals were detected on the colicomentum 3 weeks after fluorescent labelled hiPSC-MSC injection. The signal was detected both (A-a) without opening the peritoneal cavity and (A-b) on the colicomentum. (B) hiPSC-MSCs produced angiogenic and immune regulatory factors in the peritoneum cavity of rats. The levels of IGF, VEGF, HGF, PGE2, IL-4 and IL-10 in the peritoneal lavage of hiPSC-MSC injected rats was significantly increased compared with control rats. ***P<0.001. HGF, hepatocyte growth factor; IGF, insulin-like growth factor; PGE2, prostaglandin E2; hiPSC-MSCs, human induced pluripotent stem cells-mesenchymal stem cells.

Following AMI induction, the LVEF of the sham group was stable from 74.50±1.46% at week 1 to 75.19±1.93% at week 11 (Fig. 4B-a). In the PBS injection control group, LVEF declined from 44.14±4.02% at week 1 to 41.35±4.16% at week 11. In the cell injection group, LVEF increased from 46.94±2.89% at week 1 to 57.70±6.76% at week 11. A significant increase in LVEF was demonstrated when comparing the cell injection group with the PBS control group at the 11-week time point (Fig. 4B-b).

The LVFS of the sham group was stable from 46.30±4.38% at week 1 to 44±2.10% at week 11 (Fig. 4C-a). In the PBS injection control group, LVFS declined from 30.35±6.23% in week 1 to 21.27±4.73% in week 11. In the cell injection group, LVFS increased from 28.68±6.73% in week 1 to 34.45±5.79% in week 11. A significant increase was demonstrated in the LVFS of the cell injection group compared with the PBS control group at week 11 (Fig. 4C-b).

Over the 11-week experiment, four rats died in the PBS injection control group (death rate, 40%) and two rats died in the cell injection group (death rate, 20%).

hiPSC-MSC injection reduced scar size. Histological analysis was conducted 11 weeks after AMI to evaluate the percentage of scar tissue formation in the infarct area (Fig. 5A). The scar area in the PBS control group was 5.25±0.96%, which was significantly higher compared with the scar area in the cell injection group (3.33±0.88%) (Fig. 5B).

hiPSC-MSC injection enhanced vascularisation in the infarcted area. Immunohistology staining demonstrated that hiPSC-MSC injections significantly increased the number of α-SMA positive arteries in the infarcted area of the hiPSC-MSC injection group (9.42±2.45) compared with that of the PBS injection group (5.26±1.84) (Fig. 6A and B).

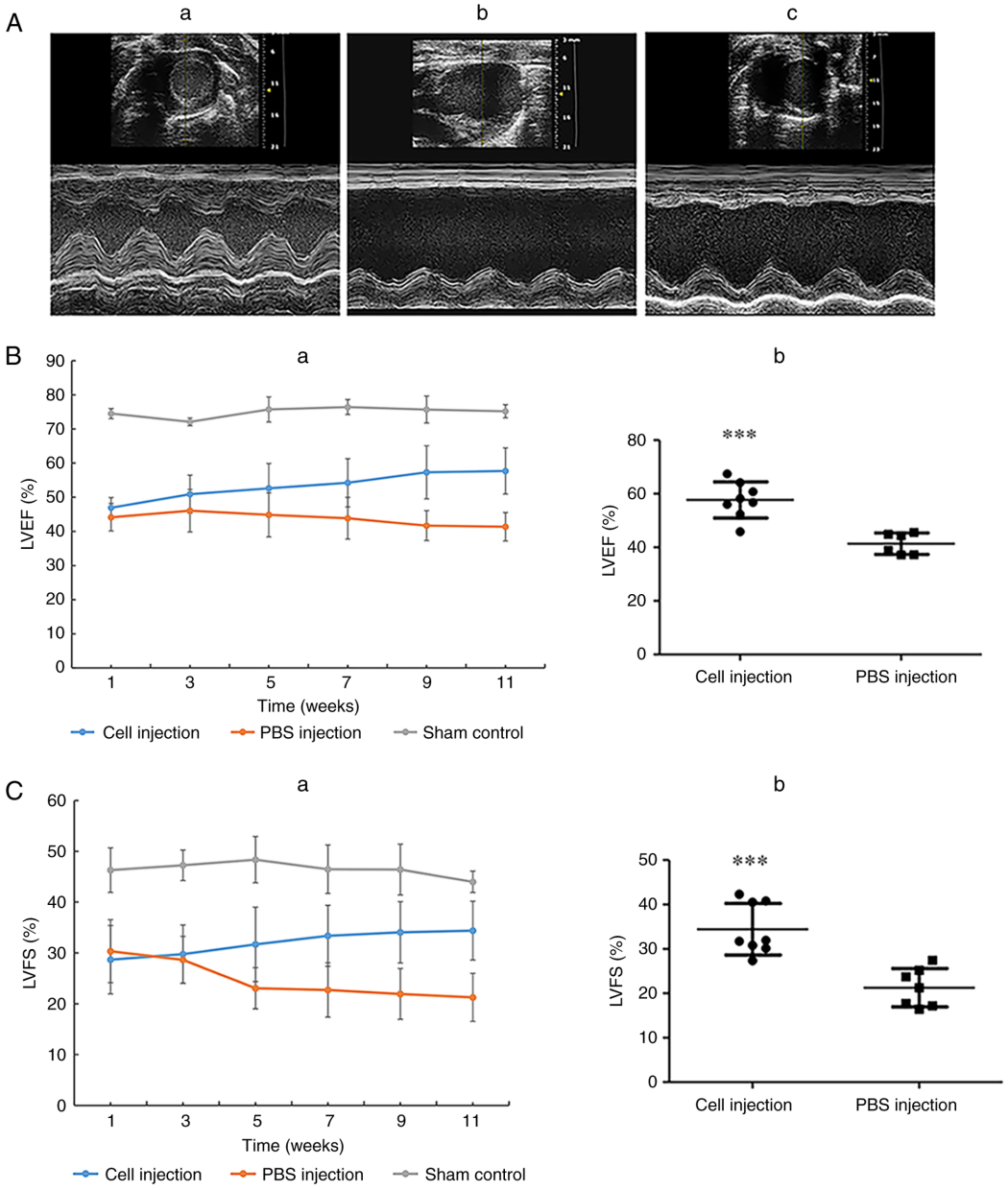

Figure 4. hiPSC-MSC injections improved cardiac function in a rat model of acute myocardial infarction. (A) Representative echocardiogram images of rat hearts in the (A-a) sham group, (A-b) PBS injection group and (A-c) hiPSC-MSC injection group. (B) LVEF measurements demonstrated that (B-a) the LVEF of the sham group was unchanged, the PBS group decreased from 44.14±4.02% to 40.35±4.16% and the hiPSC-MSC injected animals demonstrated an increase in LVEF from 46.94±2.89% to 60.33±6.29%. (B-b) A significant increase was demonstrated in the LVEF of the hiPSC-MSC injected group compared with the PBS control at week 11. (C) LVFS measurements demonstrated that (C-a) the LVFS of the sham group was stable, the LVFS of the PBS control declined from 30.35±6.23% to 21.27±4.73% and the LVFS of the hiPSC-MSC injected animals increased from 28.68±6.73% to 35.58±6.55%. (C-b) A significant difference was demonstrated in the LVFS of the hiPSC-MSC group compared with the PBS control at week 11. ***P<0.001. hiPSC-MSC, human induced pluripotent stem cells-mesenchymal stem cells; LVEF, left ventricular ejection fraction; LVFS, left ventricular fractional shortening.

hiPSC-MSC injection inhibited cell apoptosis in the infarcted area. The results of the TUNEL assay demonstrated that the apoptotic cell number in the infarcted area was significantly reduced in the cell injection group (55.5±11.98 cells/hpf) compared with the PBS injection control group (87.26±19.68 cells/hpf) (Fig. 7A and B).

Discussion

Due to their ability to release soluble immune modulators and angiogenic factors, MSCs have been investigated as a candidate for the treatment of ischemic myocardial disease for >10 years. However, there are still a number of obstacles hampering the use of MSCs in clinic treatment, such as the lack of methods for the rapid, high quality production of MSCs and issues concerning the safe and effective administration of MSCs to patients without the therapeutic efficacy being affected. hiPSCs have been regarded as a potential stem cell source for cell therapies. hiPSCs can be obtained without the consideration of ethical constraints as they are not primary cells isolated from human tissue and can be rapidly propagated *in vitro*, thus providing a unified starting point for downstream cell induction at a large scale (32). In the present study, MSC-like cells were rapidly obtained from hiPSCs using CHIR99021 and TGF-β combined

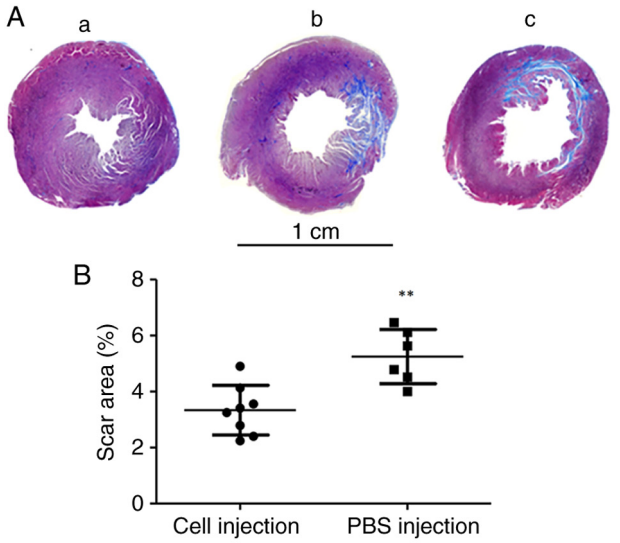

Figure 5. Human induced pluripotent stem cells-mesenchymal stem cell injection reduced scar size. (A) Masson's Trichrome staining demonstrated that acute myocardial infarction caused scar formation in the infarct area (scale bar, 1 cm). (A-a) Sham group, (A-b) cell injection group and (A-c) PBS injection group. The blue staining indicated scar tissue whereas the pink stained areas were viable tissue. (B) The scar area in the PBS control group was significantly higher at 8.8±2.28% compared with the cell injection group which demonstrated a scar area of 4.13±0.89%. **P<0.01.

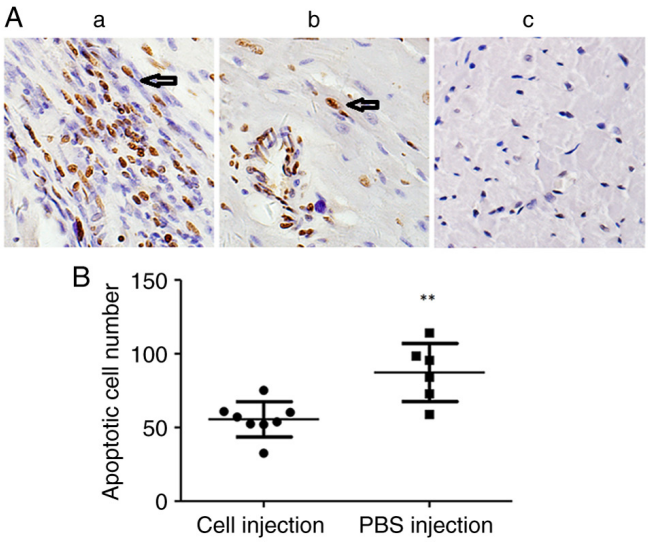

Figure 7. hiPSC-MSC injection inhibited cell apoptosis in the infarcted area. (A) TUNEL assay of apoptotic cells in the (A-a) PBS injection group, (A-b) cell injection group and (A-c) sham group. Magnification, x400. (B) The number of apoptotic cells in the infarcted area was significantly reduced in the hiPSC-MSC injection group (55.5±11.98 cells/hpf) compared with the PBS injection control group (87.26±19.68 cells/hpf). **P<0.01. hiPSC-MSC, human induced pluripotent stem cells-mesenchymal stem cells; hpf, high-powered field.

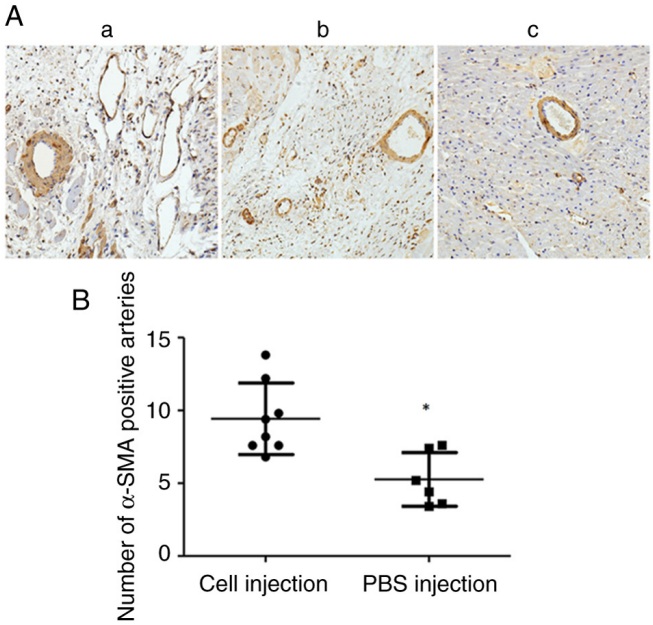

Figure 6. hiPSC-MSC injection enhanced vascularisation in the infarcted area. (A) Detection of α-SMA positive arteries in the (A-a) cell injection group, (A-b) PBS injection group and (A-c) sham group. Magnification, x200. (B) hiPSC-MSC injections significantly increased the number of α-SMA positive arteries in the infarcted area of the hiPSC-MSC injection group (9.42±2.45) compared with the PBS-injection group (5.26±1.84). *P<0.05. hiPSC-MSC, human induced pluripotent stem cells-mesenchymal stem cells.

induction and IP injections of these cells improved the cardiac function of AMI model rats.

EMT is a three state transition process in which there is an intermediate partial EMT state where cells retain the characteristics of both epithelial and mesenchymal cells. Cells in this partial EMT state are more pluripotent than those which have progressed through the whole EMT process (14). A similar phenomenon has previously been reported during ETM induction of breast cancer cells (36). Consistent with the aforementioned studies, the present study demonstrated that during CHIR99021, TGF-β or CHIR99021 + TGF-β induction, the expression levels of EMT-related genes N-cadherin and Vimentin were significantly elevated, but the expression levels of the MET-related gene E-cadherin and pluripotency-related transcription factors *OCT4*, *SOX2* and *NANOG* did not decrease significantly compared with the spontaneously differentiating hiPSCs. These results suggested that CHIR99021 or TGF-β treatment initiated the process of EMT through upregulating the expression of EMT-promoting genes and these cells may be in the state of partial EMT.

TGF-β initiates EMT through SMAD-dependent or -independent signalling pathways. In the SMAD-dependent pathway, the binding of TGF-β to its receptor induces phosphorylation of SMAD-2 and SMAD-3, then the phosphorylated SMADs form complexes with SMAD-4 to transactivate the expression of SNAIL and zinc finger protein SNAI2, which represses transcription of the MET related gene E-cadherin (37). In addition, SMAD-4 can specifically bind to the promoter region of N-cadherin and Vimentin and this binding is required for the reduction of gene expression (37,38). In the SMAD-independent pathways, the TGF-β type I receptor can activate ERKs, Akt, p38 and small G proteins (39).

GSK-3 serves a key role in the regulation of EMT and inhibition of GSK-3 by CHIR99021 activation of Wnt signalling initiated human ESC differentiation (40). GSK-3 has been previously reported to participate in SMAD-3 and SMAD-4 phosphorylation and degradation (41). STAT3 promotes

SNAIL degradation through activation of GSK-3 phosphorylation, which suppresses EMT. GSK-3 inhibitors block STAT3 DNA binding activity and upregulate SNAIL expression (20).

To further clarify the mechanism involved in the EMT induction process, western blotting was performed to analyse the protein expression levels of SNAIL, SMAD-2/3, ERK-1/2 and GSK-3 in the differentiating cells. These results demonstrated that compared with the untreated control cells, the protein expression levels of SNAIL and ERK-1/2 were elevated in CHIR99021 or TGF-β treated cells. The protein expression levels of SNAIL and ERK-1/2 were significantly increased by the CHIR99021 + TGF-β combination treatment when compared with control and single reagent treated cells. These results could indicate that both SMAD-dependent and -independent singling pathways were activated in the EMT induction and the combination treatment was more effective at EMT induction compared with the single reagents tested.

Although increased protein expression levels of GSK-3 were detected in the combination treated cells, perhaps due to the significant upregulation of SNAIL and ERK-1/2, EMT promotion in the differentiating cells was not affected. Similar results have previously been reported Li *et al* (41) who showed that a GSK-3β inhibitor preserved the activity of SNAIL and prevented Vimentin degradation. Vincent *et al* (20) previously reported that a GSK-3β inhibitor alone did not affect the expression levels of E-cadherin but increased the protein expression levels of SNAIL and SMAD3/4.

During the process of TGF-β induced EMT, TGF-β causes cell cycle arrest that leads to the inhibition of cell proliferation (43). In the present study, when compared with the single reagent treatments, the CHIR99021 + TGF-β combined treatment was more efficient in driving hiPSC cells to transform from compact large cell colonies to single migrating spindle shaped cells. However, when the concentration of CHIR99021 and TGF-β was increased to 10 μM and 20 μg/ml respectively, a decrease in the rate of cell growth and apoptosis was demonstrated in the induced cells (data not shown). As a result, a lower dosage of CHIR99021 and TGF-β was used for cell induction and the duration of induction was limited to 6 days.

In our previous study, we reported that four rounds of IV infusions of $1x10^6$ MSCs to AMI rats could improve cardiac function. The higher dosage of $2\text{-}3x10^6$ cells caused severe dyspnoea in a number of the model rats and resulted in the death of 20-50% of the animals within a short time frame, which was potentially related to pulmonary embolism (44). In the present study, in order to avoid the potential risk of small blood vessel cell embolism, IP injections were used and cell dosage was increased to $1x10^7$ cells, 10x as high as the previous IV injections in order to test the safety of high dosage IP injections. Based on our previous study, four injections were adopted in the present study and during the period from the first cell injection to the end of the experiment, no evidence of severe inflammation or tumour formation in the peritoneal cavity was observed.

Fluid exchange between the peritoneal cavity and the circulatory system is dynamic and cytokines which have been secreted into the peritoneal fluid by the intraperitoneal injected MSCs can theoretically reach every organ of the body after entering the blood circulation, including the heart. Yousefi *et al* (26) compared the therapeutic effects of IV and IP injected MSCs in treating experimental autoimmune encephalitis and reported that IP injected MSCs were more effective than IV injected MSCs. Roddy *et al* (29) reported that human MSCs were effective in reducing corneal opacity and inflammation without engraftment after either IP or IV administration following chemical injury to the rat cornea. These aforementioned studies, taken together with the present study, may indicate that IP injected MSCs exert their effects from a distance.

In the present study, the level of cytokines in the blood of rats after IP MSC injection was performed using ELISA kits, but the level of cytokines in the blood was too low to obtain reliable data (data not shown). The cytokines produced by the MSCs residing in the peritoneum were released into peritoneal fluid, exchanged into the blood circulation and were largely diluted by the blood, thus, detection of these cytokines was difficult. As a result, peritoneal fluid was collected to measure the level of the cytokines. However, the present results showed that although the serum cytokine level was low in the MSC treated rats, increased artery number and reduced apoptosis extent of myocardium cells in the infarcted area were significant comparing with the PBC injection group. Bazhanov *et al* (24) previously reported that after MSC IP injection, the level of cytokines in mouse peritoneal cavity lavage was higher compared with than that in serum.

A previous study conducted by van Dijk A *et al* (6) reported that during the first week after AMI, the resulting large scale myocardial necrosis and inflammatory cell infiltration could greatly reduce the survival rate of the injected cells, therefore, the suggested optimal time point for the administration of stem cell therapy was 1 week after the acute inflammation period. As the peritoneal cavity is separated from the infarcted heart, it is unlikely that the harsh inflammatory environment created by AMI would affect the survival of the cells injected in the peritoneal cavity to a serious extent. A previous study by Bazhanov *et al* (24) showed that the injected cells are mainly retained on the colicomentum, a result also demonstrated in the present study. Therefore, IP cell injection could be administered immediately after the AMI to cope with the onset of the tissue inflammation and cell apoptosis without inducing a pulmonary embolism.

In conclusion, the present study demonstrated that CHIR99021 and TGF-β combination treatment was a rapid and effective method to obtain MSC-like cells from hiPSCs. Additionally, multiple high dose IP injections of hiPSC-derived MSCs were a safe and effective treatment to restore the reduced cardiac function of an AMI rat model.

Acknowledgments

The authors wish to thank Dr Tiancheng Zhou at The CAS Key Laboratory of Regenerative Biology, South China Institute for Stem Cell Biology and Regenerative Medicine, Guangzhou Institutes of Biomedicine and Health, Chinese Academy of Sciences, Guangzhou 510530, P.R. China for kindly providing the PBMC-5 human iPSC cell line.

Funding

This work was supported by The National Natural Science Foundation of China (grant no. 82001654), The Shenzhen

Science and Technology Innovation Committee Basic Science Research Grant (grant no. JCYJ20190809094819102), The Guangzhou Sijiahui Tumour Prevention Foundation (grant no. GASTO-22-01-002), The Shenzhen Biomedical Industry Major Public Service Platform and Core Technology Research Special Support Plan (grant no. XMHT20220104048) and The Shenzhen Key Medical Discipline Construction Fund (grant no. SZXK051).

Availability of data and materials

The datasets used and/or analysed during the current study are available from the corresponding author on reasonable request.

Authors' contributions

YuZ and YaZ confirm the authenticity of all the raw data. YuZ prepared the acute myocardium infarction model and tissue specimens and conducted cardiac function evaluation. YaZ performed EMT-induction, flow cytometry analysis, western blotting, RT-qPCR and immunohistochemistry. AH monitored cell distribution and cytokine secretion. FM aided with acute myocardium infarction model preparation and cell injections. PC performed hiPSC culture. TL and GC designed the project, performed statistical analysis and drafted and revised the manuscript. All authors read and approved the final version of the manuscript.

Ethics approval and consent to participate

Approval for the animal experiments was granted by the Animal Ethics Committee of the Peking University & Hong Kong Science and Technology University Medical Centre (approval no. 2020-027).

Patient consent for publication

Not applicable.

Competing interests

The authors declare that they have no competing interests.

References

1. Gebler A, Zabel O and Seliger B: The immunomodulatory capacity of mesenchymal stem cells. Trends Mol Med 18: 128-134, 2012.
2. Kinnaird T, Stabile E, Burnett MS and Epstein SE: Bone-marrow-derived cells for enhancing collateral development: Mechanisms, animal data, and initial clinical experiences. Circ Res 95: 354-363, 2004.
3. Kinnaird T, Stabile E, Burnett MS, Lee CW, Barr S, Fuchs S and Epstein SE: Marrow-derived stromal cells express genes encoding a broad spectrum of arteriogenic cytokines and promote in vitro and in vivo arteriogenesis through paracrine mechanisms. Circ Res 94: 678-685, 2004.
4. van den Akker F, de Jager SC and Sluijter JP: Mesenchymal stem cell therapy for cardiac inflammation: Immunomodulatory properties and the influence of toll-like receptors. Mediators Inflamm 2013: 181020, 2013.
5. Kyurkchiev D, Bochev I, Ivanova-Todorova E, Mourdjeva M, Oreshkova T, Belemezova K and Kyurkchve S: Secretion of immunoregulatory cytokines by mesenchymal stem cells. World J Stem Cells 6: 552-570, 2014.
6. van Dijk A, Naaijkens BA, Jurgens WJ, Nalliah K, Sairras S, van der Pijl RJ, Vo K, Vonk AB, van Rossum AC, Paulus WJ, *et al*: Reduction of infarct size by intravenous injection of uncultured adipose derived stromal cells in a rat model is dependent on the time point of application. Stem Cell Res 7: 219-229, 2011.
7. Vela DC, Silva GV, Assad JA, Sousa AL, Coulter S, Fernandes MR, Perin EC, Willerson JT and Buja LM: Histopathological study of healing after allogenic mesenchymal stem cell delivery in myocardial infarction in dogs. J Histochem Cytochem 57: 167-176, 2009.
8. Perin EC, Tian M, Marini FC III, Silva GV, Zhang Y, Baimbridge F, Quan X, Fernandes MR, Gahremanpour A, Young D, *et al*: Imaging long-term fate of intramyocardially implanted mesenchymal stem cells in a porcine myocardial infarction model. PLoS One 6: e22949, 2011.
9. Williams AR and Hare JM: Mesenchymal stem cells: Biology, pathophysiology, translational findings, and therapeutic implications for cardiac disease. Circ Res 109: 923-940, 2011.
10. Kern S, Eichler H, Stoeve J, Klüter H and Bieback K: Comparative analysis of mesenchymal stem cells from bone marrow, umbilical cord blood, or adipose tissue. Stem Cells 24: 1294-1301, 2006.
11. Zhou S, Greenberger JS, Epperly MW, Goff JP, Adler C, Leboff MS and Glowacki J: Age-related intrinsic changes in human bonemarrow-derived mesenchymal stem cells and their differentiation to osteoblasts. Aging Cell 7: 335-343, 2008.
12. Zhang L, Wei Y, Chi Y, Liu D, Yang S, Han Z and Li Z: Two-step generation of mesenchymal stem/stromal cells from human pluripotent stem cells with reinforced efficacy upon osteoarthritis rabbits by HA hydrogel. Cell Biosci 11: 6, 2021.
13. Katsuno Y and Derynck R: Epithelial plasticity, epithelial-mesenchymal transition, and the TGF-β family. Dev Cell 56: 726-746, 2021.
14. Nieto MA, Huang RY, Jackson RA and Thiery JP: EMT: 2016. Cell 166: 21-45, 2016.
15. Tian XJ, Zhang H and Xing J: Coupled reversible and irreversible bistable switches underlying TGFβ-induced epithelial to mesenchymal transition. Biophys J 105: 1079-1089, 2013.
16. Bhatia S, Monkman J, Blick T, Pinto C, Waltham M, Nagaraj SH and Thompson EW: Interrogation of phenotypic plasticity between epithelial and mesenchymal states in breast cancer. J Clin Med 8: 893, 2019.
17. Tripathi S, Chakraborty P, Herbert L and Jolly MK: A mechanism for epithelial-mesenchymal heterogeneity in a population of cancer cells. PLoS Comput Biol 16: e1007619, 2020.
18. Fan X, Zhao Z, Wang D and Xiao J: Glycogen synthase kinase-3 as a key regulator of cognitive function. Acta Biochim Biophys Sin (Shanghai) 52: 219-230, 2020.
19. Zhou BP, Deng J, Xia W, Xu J, Li YM, Gunduz M and Hung MC: Dual regulation of snail by GSK-3beta-mediated phosphorylation in control of epithelial-mesenchymal transition. Nat Cell Biol 6: 931-940, 2004.
20. Vincent T, Neve EP, Johnson JR, Kukalev A, Rojo F, Albanell J, Pietras K, Virtanen I, Philipson L, Leopold PL, *et al*: A SNAIL1-SMAD3/4 transcriptional repressor complex promotes TGF-beta mediated epithelial-mesenchymal transition. Nat Cell Biol 11: 943-950, 2009.
21. Nguyen TMX, Vegrichtova M, Tlapakova T, Krulova M and Krylov V: Epithelial-mesenchymal transition promotes the differentiation potential of *xenopus tropicalis* immature sertoli cells. Stem Cells Int 2019: 8387478, 2019.
22. Zanetti A, Grata M, Etling EB, Panday R, Villanueva FS and Toma C: Suspension-expansion of bone marrow results in small mesenchymal stem cells exhibiting increased transpulmonary passage following intravenous administration. Tissue Eng Part C Methods 21: 683-692, 2015.
23. Galipeau J and Sensébé L: Mesenchymal stromal cells: Clinical challenges and therapeutic opportunities. Cell Stem Cell 22: 824-833, 2018.
24. Bazhanov N, Ylostalo JH, Bartosh TJ, Tiblow A, Mohammadipoor A, Foskett A and Prockop DJ: Intraperitoneally infused human mesenchymal stem cells form aggregates with mouse immune cells and attach to peritoneal organs. Stem Cell Res Ther 7: 27, 2016.
25. Lee RH, Pulin AA, Seo MJ, Kota DJ, Ylostalo J, Larson BL, Semprun-Prieto L, Delafontaine P and Prockop DJ: Intravenous hMSCs improve myocardial infarction in mice because cells embolized in lung are activated to secrete the anti-inflammatory protein TSG-6. Cell Stem Cell 5: 54-63, 2009.
26. Yousefi F, Ebtekar M, Soleimani M, Soudi S and Hashemi SM: Comparison of in vivo immunomodulatory effects of intravenous and intraperitoneal administration of adipose-tissue mesenchymal stem cells in experimental autoimmune encephalomyelitis (EAE). Int Immunopharmacol 17: 608-616, 2013.

27. Cheng K, Rai P, Plagov A, Lan X, Kumar D, Salhan D, Rehman S, Malhotra A, Bhargava K, Palestro CJ, *et al*: Transplantation of bone marrow-derived MSCs improves cisplatinum-induced renal injury through paracrine mechanisms. Exp Mol Pathol 94: 466-473, 2013.
28. Castelo-Branco MT, Soares ID, Lopes DV, Buongusto F, Martinusso CA, do Rosario A Jr, Souza SA, Gutfilen B, Fonseca LM, Elia C, *et al*: Intraperitoneal but not intravenous cryopreserved mesenchymal stromal cells home to the inflamed colon and ameliorate experimental colitis. PLoS One 7: e33360, 2012.
29. Roddy GW, Oh JY, Lee RH, Bartosh TJ, Ylostalo J, Coble K, Rosa RH Jr and Prockop DJ: Action at a distance: Systemically administered adult stem/progenitor cells (MSCs) reduce inflammatory damage to the cornea without engraftment and primarily by secretion of TNF-α stimulated gene/protein 6. Stem Cells 29: 1572-1579, 2011.
30. Choi H, Lee RH, Bazhanov N, Oh JY and Prockop DJ: Anti-inflammatory protein TSG-6 secreted by activated MSCs attenuates zymosan-induced mouse peritonitis by decreasing TLR2/NF-κB signaling in resident macrophages. Blood 118: 330-338, 2011.
31. Zhang J, Tian XJ, Zhang H, Teng Y, Li R, Bai F, Elankumaran S and Xing J: TGF-β-induced epithelial-to-mesenchymal transition proceeds through stepwise activation of multiple feedback loops. Sci Signal 7: ra91, 2014.
32. Chen Q, Yang W, Wang X, Li X, Qi S, Zhang Y and Gao MQ: TGF-β1 induces EMT in bovine mammary epithelial cells through the TGFβ1/smad signaling pathway. Cell Physiol Biochem 43: 82-93, 2017.
33. Jin W, He Y, Li T, Long F, Qin X, Yuan Y, Gao G, Shakhawat HM, Liu X, Jin G and Zhou Z: Zhou. Rapid and robust derivation of mesenchymal stem cells from human pluripotent stem cells via temporal induction of neuralized ectoderm. Cell Biosci 12: 31, 2022.
34. Livak KJ and Schmittgen TD: Analysis of relative gene expression data using real-time quantitative PCR and the 2(-Delta Delta C(T)) method. Methods 25: 402-408, 2001.
35. Kilkenny C, Browne W, Cuthill IC, Emerson M and Altman DG; NC3Rs Reporting Guidelines Working Group: Animal research: Reporting in vivo experiments: The ARRIVE guidelines. Br J Pharmacol 160: 1577-1579, 2010.
36. Zhang S, Tang Z, Qing B, Tang R, Duan Q, Ding S and Deng D: Valproic acid promotes the epithelial-to-mesenchymal transition of breast cancer cells through stabilization of Snail and transcriptional upregulation of Zeb1. Eur J Pharmacol 865: 172745, 2019.
37. Yang H, Wang L, Zhao J, Chen Y, Lei Z, Liu X, Xia W, Guo L and Zhang HT: TGF-β-activated SMAD3/4 complex transcriptionally upregulates N-cadherin expression in non-small cell lung cancer. Lung Cancer 87: 249-257, 2015.
38. Rogel MR, Soni PN, Troken JR, Sitikov A, Trejo HE and Ridge KM: Vimentin is sufficient and required for wound repair and remodeling in alveolar epithelial cells. FASEB J 25: 3873-3883, 2011.
39. Dubon MJ, Yu JY, Choi S and Park KS: Transforming growth factor β induces bone marrow mesenchymal stem cell migration via noncanonical signals and N-cadherin. J Cell Physiol 233: 201-213, 2018.
40. Setiawan M, Tan XW, Goh TW, Hin-Fai Yam G and Mehta JS: Inhibiting glycogen synthase kinase-3 and transforming growth factor-β signaling to promote epithelial transition of human adipose mesenchymal stem cells. Biochem Biophys Res Commun 490: 1381-1388, 2017.
41. Patel P and Woodgett JR: Glycogen synthase kinase 3: A kinase for all pathways? Curr Top Dev Biol 123: 277-302, 2017.
42. Li CH, Liu CW, Tsai CH, Peng YJ, Yang YH, Liao PL, Lee CC, Cheng YW and Kang JJ: Cytoplasmic aryl hydrocarbon receptor regulates glycogen synthase kinase 3 beta, accelerates vimentin degradation, and suppresses epithelial–mesenchymal transition in non-small cell lung cancer cells. Arch Toxicol 91: 2165-2178, 2017.
43. Song J and Shi W: The concomitant apoptosis and EMT underlie the fundamental functions of TGF-β. Acta Biochim Biophys Sin (Shanghai) 50: 91-97, 2018.
44. Guo S, Zhang Y, Zhang Y, Meng F, Li M, Yu Z, Chen Y and Cui G: Multiple intravenous injections of valproic acid-induced mesenchymal stem cell from human-induced pluripotent stem cells improved cardiac function in an acute myocardial infarction rat model. Biomed Res Int 2020: 2863501, 2020.